Chemical Engineering Journal 162 (2010) 430–435

Contents lists available at ScienceDirect

Chemical Engineering Journal

journal homepage: www.elsevier.com/locate/cej

Short communication

Morphology and structure of electrospun $CoFe_2O_4$/multi-wall carbon nanotubes composite nanofibers

F.R. Lamastra[a,*], F. Nanni[a,b], L. Camilli[b], R. Matassa[c], M. Carbone[b], G. Gusmano[a,b]

[a] Italian Interuniversity Consortium on Materials Science and Technology (INSTM), Research Unit Roma Tor Vergata, Via della Ricerca Scientifica, 00133 Rome, Italy
[b] University of Rome "Tor Vergata", Department of Chemical Science and Technology, Via della Ricerca Scientifica, 00133 Rome, Italy
[c] Centro Grandi Apparecchiature, University of Palermo, Via F. Marini 14, 90128 Palermo, Italy

ARTICLE INFO

Article history:
Received 19 January 2010
Received in revised form 3 May 2010
Accepted 12 May 2010

Keywords:
Carbon nanotubes
Cobalt ferrite
Nanofiber
Electrospinning
Morphology

ABSTRACT

$CoFe_2O_4$/multiwall carbon nanotubes (MWCNTs) composite nanofibers were produced by electrospinning a dispersion of MWCNTs in a solution of polyvinylpyrrolidone, iron(III) nitrate nonahydrate, cobalt (II) acetate tetrahydrate, absolute ethanol and H_2O. Microstructure was examined by scanning electron microscopy (SEM) and high resolution transmission electron microscopy (HR-TEM). Thermal behaviour was studied by thermogravimetry and differential thermal analysis (TG-DTA) and phase analysis of calcined fibers was performed by X-ray diffraction (XRD). Upon thermal treatment at 450 °C defect-free, randomly oriented composite fibers having a mean diameter of 60 ± 10 nm were obtained. The results show that the presence of MWCNTs does not affect the spinel cubic phase formation.

1. Introduction

Due to the high coercive force, hardness, chemical stability and moderate saturation magnetization, $CoFe_2O_4$ materials are widely employed in magnetic and magnetooptical recording devices, high performance electromagnetic and spintronic devices [1,2]. Moreover the high complex permeability at a wide frequency range made the material highly efficient as magnetic filler in microwave absorbers [3]. The electromagnetic absorbing performance of a material, in fact, is directly related to its intrinsic electromagnetic properties, as complex permittivity and permeability, as well as to geometrical features as thickness. Generally speaking, wave absorption is enhanced if magnetic and/or dielectric losses are promoted. Many papers [4,5] report CNTs to be extremely efficient filler in polymer composites to gain good microwave absorption, due to their conductivity that increases dielectric losses. On the other hand, $CoFe_2O_4$ for what previously reported, is an ideal candidate as magnetic filler of polymer composites for this application [6]. Therefore it seems of great interest the possibility to synthesize a nanofiller that can embody CNT and ferrite advantages [7].

Recently a growing attention is devoted to produce one-dimensional (1D) magnetic nanomaterials i.e. nanotubes, nanowires, nanofibers, and nanobelts due to their enhanced magnetic properties.

Such systems are gaining interest particularly as magnetic fillers of polymers and resins in shielding/absorbing systems. This is due to the fact that, by comparison with their analogous particle-like fillers, well dispersed 1D nanomaterials form a more extended network that behave as a mesh intercepting the electromagnetic radiation [8].

The synthesis of $CoFe_2O_4$ in form of nanowire arrays by template-electrodeposition method and further oxidization has been reported in [9]. Still concerning the synthesis of magnetic $CoFe_2O_4$ nanowires it was evidenced in [10] the use of carbon nanotubes as a template for the mild synthesis. Nevertheless only recently $CoFe_2O_4$ nanofibers were obtained by calcination of electrospun precursors i.e. cobalt nitrate/ferric nitrate/PVAc [1], cobalt acetate/ferric nitrate/PVP [11] and cobalt nitrate/ferric nitrate/PVP [12,13] composite fibers. Electrospinning is an extremely flexible, low cost and easily industrial exploiting process to fabricate continuous nanofibers from a huge range of materials [14].

In this work, to the best of our knowledge, $CoFe_2O_4$/multi-wall carbon nanotubes (MWCNTs) composite nanofibers were successfully produced for the first time. Till now CNTs were embedded in numerous polymeric fibres [15] such as PS [16], PVA [17] and only in few types of ceramic nanofibres as SnO_2 [18], TiO_2 [19] and Al_2O_3 [20]. The prepared nanofibrous composites are expected to exhibit an improved microwave absorption due to the better match between the dielectric loss and magnetic loss, which originates from the combination of paramagnetic CNTs and ferrimagnetic $CoFe_2O_4$, as suggested by Che et al. in [3] in relation to CNTs/$CoFe_2O_4$ particles nanocomposites obtained *via* CVD.

* Corresponding author. Tel.: +39 06 72594273; fax: +39 06 72594328.
E-mail address: lamastra@scienze.uniroma2.it (F.R. Lamastra).

1385-8947/$ – see front matter © 2010 Elsevier B.V. All rights reserved.
doi:10.1016/j.cej.2010.05.025

2. Experimental

2.1. Preparation of $CoFe_2O_4$ and $CoFe_2O_4$/MWCNTs nanofibrous mats

$CoFe_2O_4$ precursor solution was prepared dissolving 2 g of polyvinylpyrrolidone (PVP, *Aldrich*, MW 1300000), 2 g of iron(III) nitrate nonahydrate ($Fe(NO_3)_3{\cdot}9H_2O$ 99.99%, *Aldrich*) and 0.6104 g of cobalt (II) acetate tetrahydrate ($Co(CH_3COO)_2 \cdot 4H_2O$, *Aldrich*) in a mixed solvent consisting on 20 mL of absolute ethanol and 8 mL of H_2O, under magnetic stirring for 12 h. Multi-wall carbon nanotubes (MWCNTs, NT3100, Nanocyl, Belgium), with an average diameter of 9.5 nm and average length of 1.5 μm, were dispersed in ethanol (7 ml) under high frequency sonication (Sonics VibraCell) using a 52 wt.% block copolymer solution in 1-methoxy-2-propyl acetate (Disperbyk-2150, BYK-CHEMIE) as dispersant. The amount of nanotubes used was 1 wt% with respect to $CoFe_2O_4$. After 30 min of sonication the dispersion was added to the $CoFe_2O_4$ precursor solution previously prepared. The resulting mixture was stirred for 10 minutes and sonicated for 5 minutes before electrospinning. For comparison PVP and $CoFe_2O_4$ precursor solutions were electrospun too. Viscosity of solution/suspension was measured at 25 °C by a digital viscosimeter (*Brookfield DV-II +, Middleboro, MA, USA*) using a SC4-21 spindle at 20 rpm. Conductivities were evaluated at 25 °C (CDM230, *Analitica De Mori, Italy*).

Solution/suspension was poured in a glass syringe (*Hamilton, Carlo Erba*) equipped with a 20 G needle, fixed in a digitally controlled syringe pump (*KD Scientific, MA, USA*). The needle was connected to a high-voltage supply (*Spellman, Model SL 30, NY, USA*) able to generate DC voltages up to 30 kV. A grounded aluminium target (diameter 10 cm) was used to collect electrospun mats.

PVP and $CoFe_2O_4$ precursor solutions were electrospun in air in the following conditions: tension 15 kV, needle-target distance 6 cm, feed rate 1 ml/h. The processing parameters adopted for $CoFe_2O_4$/MWCNTs precursor suspension were: tension 15 kV, needle-target distance 8 cm, feed rate 0.7 ml/h. The resulting mats were designed as PVP, PVP/$CoFe_2O_4$ and PVP/$CoFe_2O_4$/MWCNTs. In order to remove the polymeric component, PVP/$CoFe_2O_4$ and PVP/$CoFe_2O_4$/MWCNTs were finally calcined in air at 450-600 °C and 450 °C for 1 h, respectively, heating and cooling rate being 2 °C/min.

2.2. Characterisation of $CoFe_2O_4$ and $CoFe_2O_4$/MWCNTs nanofibrous mats

Morphology was examined by Field Emission-Scanning Electron Microscopy (FEG-SEM, *Leo Supra 35*) on gold sputtered samples and the average fiber diameter was evaluated using a CAD software (average on ~ 100 fibers selection). The thermal behaviour of as-spun mats was investigated by simultaneous TG-DTA analysis (*Netzsch STA 409*) performed in the following conditions: air flow 80 cm^3/min, peak temperature 1250 °C, heating rate 5 °C/min, sample weight about 60 mg. Thermal behaviour of MWCNTs was also analysed by TG-DTA.

Phase analysis of calcined electrospun mats was performed by means of X-ray diffraction (XRD, *Philips X'Pert 1710*, Cu-Kα radiation λ=1.5405600 Å, 10-80° 2θ, step size 0.020°, time per step 2 s, scan speed 0.005°/s). The average crystallite size (τ) of all calcined samples was evaluated by means of Scherrer's equation (1):

$$\tau = \frac{K\lambda}{\beta \cos\theta} \quad (1)$$

where K is the shape factor taken as 0.89, λ is the X-ray wavelength, β is the full width at half maximum (FWHM) in radians, and θ is the Bragg angle [21]. From XRD spectra, also the lattice parame-

Table 1
Viscosity and conductivity of precursor solution/suspension.

Precursor solution/suspension	Viscosity (cP)	Conductivity (mS cm^{-1})
PVP	65	0.004
PVP/$CoFe_2O_4$	117	5.2
PVP/$CoFe_2O_4$/MWCNTs	1804	9.6

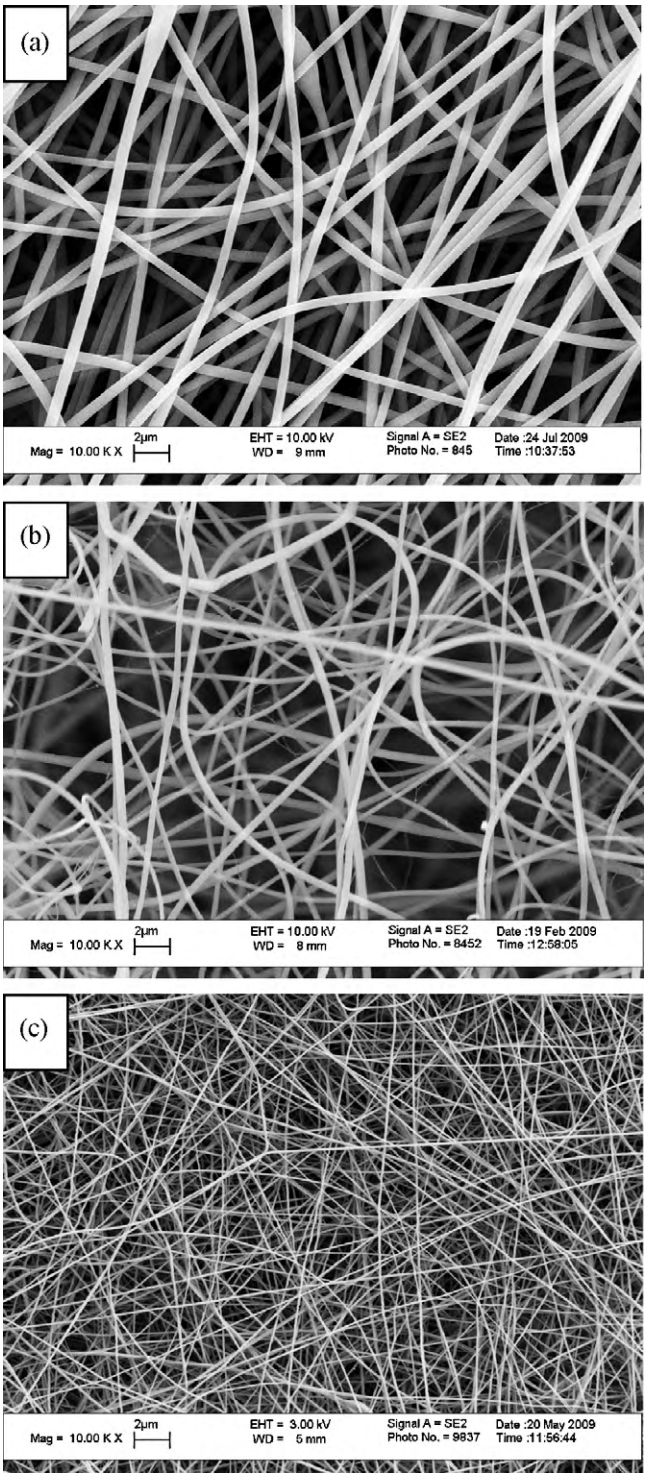

Fig. 1. SEM micrographs of electrospun mats (a) PVP (*b*) PVP/$CoFe_2O_4$ (*c*) PVP/$CoFe_2O_4$/MWCNTs.

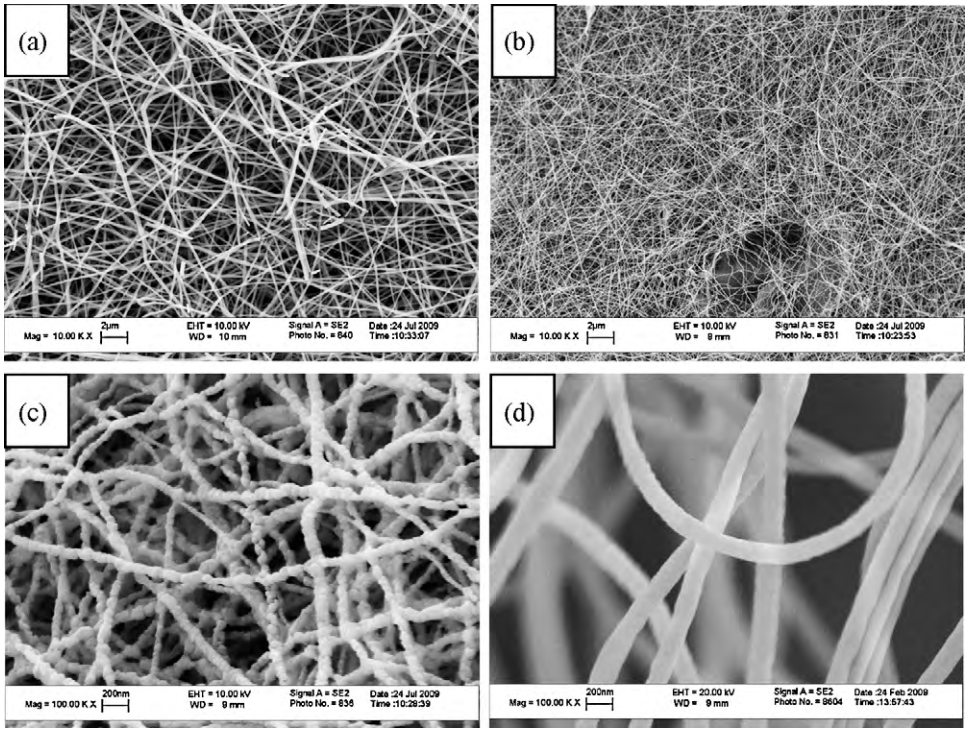

Fig. 2. SEM micrographs of $CoFe_2O_4$ nanofibers calcined at (*a*, *d*) 450 °C (b, c) 600 °C.

ters (*a*) were calculated. Both τ and *a* values were determined from (311) peak profiles of spinel cobalt ferrite, the only ones sufficiently resolved for samples calcined at 450 °C.

High Resolution-Transmission Electron Microscopy (HR-TEM) observations were performed using a JEM-2100 (JEOL, Japan) operating at 200 kV accelerating voltage, equipped with an energy dispersive X-ray spectrometer (EDS) (Oxford Instruments, UK) suited for element identification. A small quantity of $CoFe_2O_4$/MWCNTs mat was ultrasonically dispersed in ethanol and a droplet of the suspension was deposited onto an holey carbon film on 300 mesh copper grid. To further investigate the detailed structure of the $CoFe_2O_4$ particle, the high-resolution image of the particle was chosen for Fourier Transfer (FT) and Inverse Fourier Transfer (IFT) treatments of selected nano-area using DigitalMicrograph GATAN software.

3. Results and discussion

3.1. Morphology of electrospun mats

Parameters affecting fibers formation *via* electrospinning may be classified into solution parameters (i.e. surface tension, viscosity, conductivity) and processing conditions (i.e. applied voltage, needle-target distance, feed rate, ambient parameters, etc) [22]. Although the latters have some influence in fiber morphology and size, nevertheless they are less significant than solution parameters as electrical conductivity and viscosity. In particular, high conductivity and low viscosity solutions lead to the formation of fibers with very small diameter [22]. Thus viscosity and conductivity of precursor solution/suspension were carefully checked to perform a strict control on the electrospinning process. As expected, it was found that the electric conductivity in the ceramic spinnable solution/suspension is far higher than that of the PVP solution (Table 1), the effect being even more noteworthy in the case of PVP/$CoFe_2O_4$/MWCNTs system, due to the addition of the electrically conductive filler. Nevertheless, the presence of MWCNTs leads

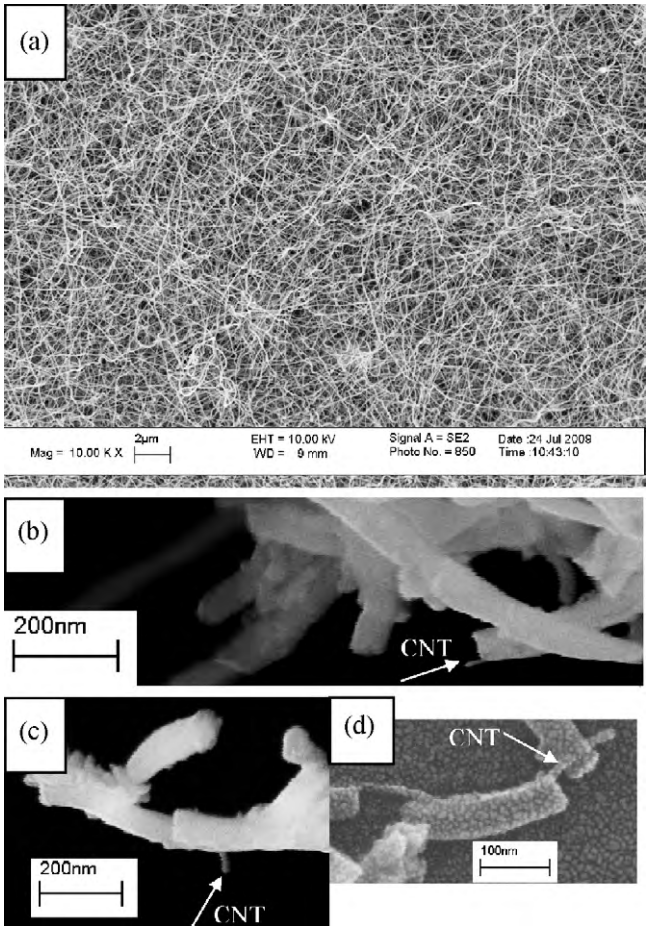

Fig. 3. SEM micrographs of $CoFe_2O_4$/MWCNTs nanofibers calcined at 450 °C.

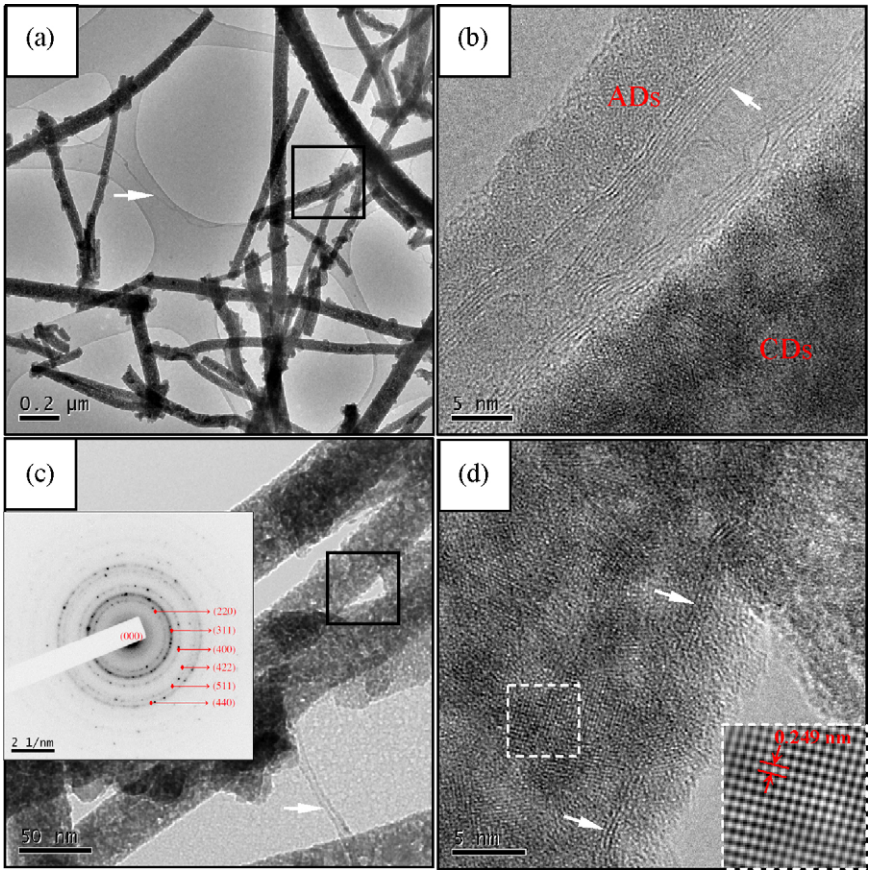

Fig. 4. Bright field TEM images of $CoFe_2O_4$/MWCNTs nanofibers, the white narrows indicate the presence of MWCNTs. (a) Low magnification TEM image of $CoFe_2O_4$ nanofibers with diameters from 40 to 65 nm. (b) HR-TEM image of the square black line area shown in (a). The MWCNT is sandwiched between an amorphous domains (ADs) and a crystalline domains (CDs). (c) Low magnification TEM image of $CoFe_2O_4$ nanofibers of different region and corresponding SAED pattern (insert frame) (d) HR-TEM image of the square black line area shown in (c). The MWCNT embedded into nanofibre is displayed. Inset shows a IFT image of a $CoFe_2O_4$ crystalline domain (square white dot line), yielding a directly structural information with about 0.249 nm lattice fringes characteristic for the $CoFe_2O_4$ (311) plane.

to a remarkable increase of viscosity that de facto limited the benefit of increasing conductivity (Table 1).

SEM micrographs of electrospun mats are presented in Figs. 1–3. All samples consisted of defect-free, randomly oriented fibers of fairly uniform diameter, forming a porous, highly interconnected architecture. The average diameters of neat PVP, PVP/$CoFe_2O_4$ and PVP/$CoFe_2O_4$/MWCNTs nanofibers were found to be 500 ± 100 nm, 460 ± 100 nm and 100 ± 10 nm, respectively (Fig. 1a-c). The remarkable smaller fiber size of PVP/$CoFe_2O_4$/MWCNTs mat has to be associated with the higher conductivity of the electrospun suspension (Tab.1). Calcination of PVP/$CoFe_2O_4$ at 450 °C and 600 °C results in the formation of ceramic nanofibers with average diameter of respectively 160 ± 30 nm and 60 ± 10 nm (Fig. 2a-d), being the significant reduction of fiber size due to the removal of the polymeric component. Samples calcined at lower and higher temperatures present markedly different microstructures, being the former characterised by smooth surface fibers (Fig. 2d), while the latter shows a necklace-like structure consisted of linked crystalline particles or crystallites (Fig. 2c). Such event has most probably to be correlated to the different degree of crystallisation reached during thermal treatment, as confirmed by the XRD spectra (see paragraph 3.2). $CoFe_2O_4$/MWCNTs were calcined only at 450 °C, since at higher temperature CNT combustion occurs (see paragraph 3.2). The resulting fibers present an average diameter of 60 ± 10 nm (Fig. 3).

Transmission electron microscopy observations (Fig. 4) provide uniform diameters of the nanofibers from 40 to 65 nm with lengths up to micrometers, as shown in Fig. 4a. Moreover, the morphological study reveals several nanofibers with a slightly rougher surfaces, depending from the calcination temperature that affects crystal growth and the size diameters of the nanofibers (Figs. 3 and 4c). Low magnification TEM images show MWCNTs not completely embedded into the nanofibers (Fig. 4a and c). An accurate observation at higher magnification of the specimen allowed to display part of MWCNTs within the nanofibres. The mass-thickness and phase contrasts due to the presence of $CoFe_2O_4$ crystalline domains partially hide the multi walls of the CNTs embedded into the nanofibers because of its diffraction contrast that dominate on the multi walls of the carbon nanotube [23]. Multi walls of the CNT embedded into the nanofiber are shown in Figure 4d.

HR-TEM image clearly shows that MWCNTs are well aligned to the nanofiber axis (Fig. 4b), in agreement with what reported in literature in similar systems [19]. MWCNTs were found to be often confined at the borderline of the $CoFe_2O_4$ nanofiber between rough surface amorphous domain (AD) and inner grains of the crystalline domains (CDs).

The selected area electron diffraction (SAED) pattern (insert frame in Fig. 4c) of nanofibers shows dense spotty ring patterns with interplanar spacings (d_{hkl}) revealing the crystalline spinel $CoFe_2O_4$ structure (JCPDS 03-0864). The diffraction rings can be indexed to (220), (311), (400), (422), (511) and (440) planes and the measured lattice constant agrees with that determined from XRD. Diffraction from MWCNTs was not detected in SAED pattern.

Fig. 5.

HR-TEM analysis evidenced a porous-free grain structure densely packed along the fiber length with an average dimen-

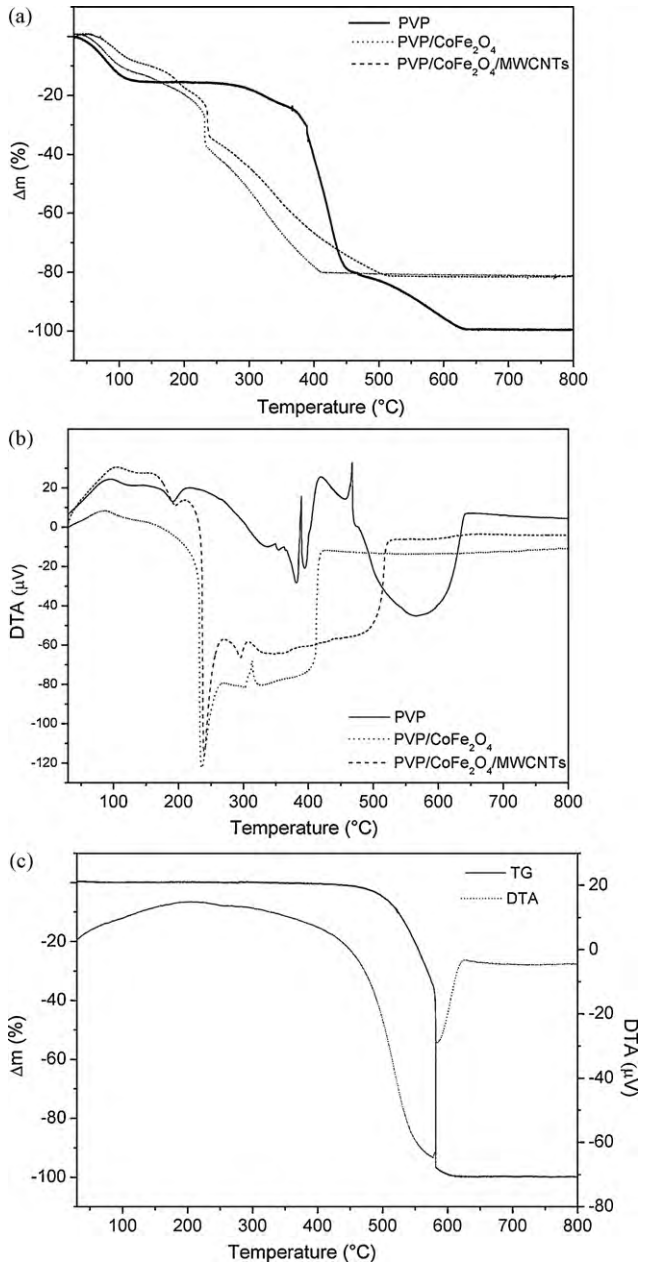

Fig. 5. (a) TG curves of PVP, PVP/$CoFe_2O_4$, PVP/$CoFe_2O_4$/MWCNTs electrospun mats (b) DTA curves of PVP, PVP/$CoFe_2O_4$, PVP/$CoFe_2O_4$/MWCNTs electrospun mats (c) TG-DTA curves of MWCNTs.

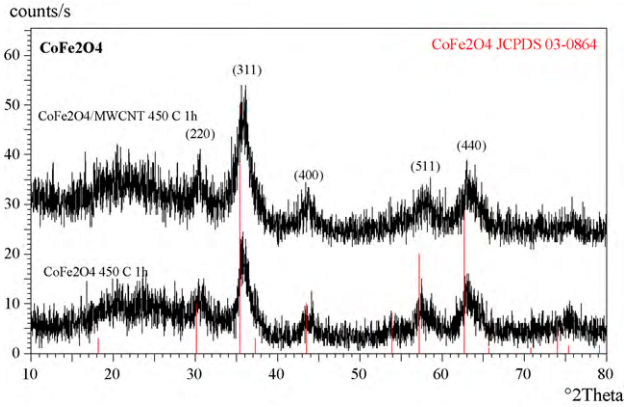

Fig. 6. XRD patterns of $CoFe_2O_4$ and $CoFe_2O_4$/MWCNTs electrospun mats calcined at 450 °C for 1h.

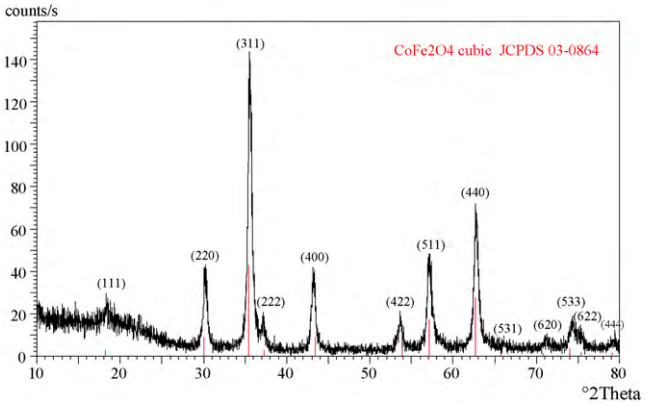

Fig. 7. XRD patterns of $CoFe_2O_4$ electrospun mat calcined at 600 °C for 1h.

sions of about 10 nm. Moreover, the IFT calculated image of the selected area of Fig. 4d (square white line) provides an estimated d-spacing between the lattice fringes of 0.249 nm corresponding to the (311) broad diffraction peak observed in the high-angle XRD pattern (Figure 6). The broadened peaks indicate that domains of stacked crystalline are very small, which can be resolved by HR-TEM technique [24].

Numerous SEM and TEM observations, carried out after the thermal treatment on different areas of the samples, indicate that only part of the MWCNTs remains confined in the fibers, while the rest is clearly visible outside them (Figs. 3 and 4). A possible explanation to justify this occurrence refers to the strong shrinkage taking place in the fibers in ceramic formation and sintering. Grains formation and arrangement during thermal treatment, in fact, can push out the nanotubes placed in the outer part of the fibers. As a result, at the end of the process, only those nanotubes that were located in the inner part of the electrospun fibers, still remains inside the ceramic fiber.

3.2. Thermal behaviour and phase analysis of electrospun mats

In Fig. 5a-b TG-DTA curves of the PVP, PVP/$CoFe_2O_4$ and PVP/$CoFe_2O_4$/MWCNTs mats are reported. All the samples showed a weight loss around 100 °C associated to the release of physically-absorbed moisture and/or of residual solvent present within the fibers. The neat PVP underwent multiple mass losses in the range 300-630 °C corresponding to the PVP combustion and decomposition [25]. The decomposition of PVP/$CoFe_2O_4$ and PVP/$CoFe_2O_4$/MWCNTs mats was completed at lower temperatures, 410 °C and 510 °C respectively. The lowering of the thermal decomposition temperatures of the PVP matrices (from 630 °C for neat PVP to 510 °C for PVP/$CoFe_2O_4$/MWCNTs and to 410 °C for PVP/$CoFe_2O_4$) might be correlated to catalytic properties of the metal centres. The slightly higher decomposition temperature of PVP/$CoFe_2O_4$/MWCNTs with respect to PVP/$CoFe_2O_4$ had to be associated to the combustion of the carbon nanotubes which occurs in the temperature range 480-580 °C (Fig. 5c).

XRD patterns of $CoFe_2O_4$ and $CoFe_2O_4$/MWCNTs calcined at 450 °C are very similar, showing that the presence of MWCNTs within the fibers does not affect the spinel cubic phase formation (Fig. 6). Annealing the $CoFe_2O_4$ mat at 600 °C led to improve crystallinity and to a larger crystallite size as shown by the increase of the intensities and decrease of the FWHM of XRD peaks (Fig. 7). Nevertheless, due to the fact that MWCNTs start to decompose at 480 °C (Fig. 5c), $CoFe_2O_4$/MWCNTs sample calcination did never exceed 450 °C. Spinel lattice parameter (a) and average crystallite size (τ) evaluated from (311) reflections of XRD patterns (Figs. 6 and 7) are reported in Table 2. The a values increase slightly with calcination

Table 2
Spinel lattice parameter (a) and average crystallite size (τ) of calcined electrospun mats determined from XRD spectra.

Sample	T (°C)	a (nm)	τ (nm)
$CoFe_2O_4$/MWCNTs	450	0.8313	12
$CoFe_2O_4$	450	0.8325	11
$CoFe_2O_4$	600	0.8371	20

temperature and for $CoFe_2O_4$ and $CoFe_2O_4$/MWCNTs calcined at 450 °C are not significantly different, confirming that the presence of MWCNTs within the fibers does not affect the spinel structure.

Moreover, the values obtained at the lower temperature are slightly smaller than that reported for $CoFe_2O_4$ (a = 0.8377 nm) in the standard data (JCPDS: 03-0864). For $CoFe_2O_4$ sample calcined at 600 °C the value calculated was in good agreement with JCPDS card 03-0864. As expected, average crystallite size increases with calcination temperature, the presence of the nanotubes seems to have no influence on it. The value obtained for the composite fibrous sample agrees with the average crystallite size observed in TEM images.

4. Conclusions

Randomly oriented $CoFe_2O_4$/MWCNTs composite nanofibers forming a porous, highly interconnected architecture were successfully produced by electrospinning. The amount of nanotubes used was 1 wt% with respect to $CoFe_2O_4$. The average diameter of as-spun fibers was 100 ± 10 nm. Upon thermal treatment at 450 °C composite nanofibers having a mean diameter of 60 ± 10 nm were obtained. The insertion of nanotubes within $CoFe_2O_4$ fibers was confirmed by SEM and TEM analysis, even if CNTs only partially remain confined within the ceramic fibres, while some part of them came out during thermal treatment. For comparison $CoFe_2O_4$ nanofibers were prepared. The average diameter of neat ceramic fibers calcinated at 450 °C and 600 °C was 160 ± 30 nm and 60 ±10 nm, respectively. X-ray analysis performed on calcined ceramic and composite nanofibers showed that the presence of the nanotubes does not affect the spinel cubic phase formation and structure.

References

[1] Y.-W. Ju, J.-H. Park, H.-R. Jung, S.-J. Cho, W.-J. Lee, Fabrication and characterization of cobalt ferrite ($CoFe_2O_4$) nanofibers by electrospinning, Mater. Sci. Eng. B 147 (2008) 7–12.
[2] L. Zhao, H. Zhang, Y. Xing, S. Song, S. Yu, W. Shi, X. Guo, J. Yang, Y. Lei, F. Cao, Studies on the magnetism of cobalt ferrite nanocrystals synthesized by hydrothermal method, J. Solid State Chem. 181 (2008) 245–252.
[3] R.C. Che, C.Y. Zhi, C.Y. Liang, X.G. Zhou, Fabrication and microwave absorption of carbon nanotubes/$CoFe_2O_4$ spinel nanocomposite, Appl. Phys. Lett. 88 (2006) 033105.
[4] Y. Li, C. Chen, S. Zhang, Y. Ni, J. Huang, Electrical conductivity and electromagnetic interference shielding characteristics of multiwalled carbon nanotube filled polyacrylate composite films, Appl. Surf. Sci. 254 (2008) 5766–5771.
[5] F. Nanni, P. Travaglia, M. Valentini, Effect of carbon nanofibres dispersion on the microwave absorbing properties of CNF/epoxy composites, Compos. Sci. Technol. 69 (2009) 485–490.
[6] H. Dong, A. Meininger, K.S. Moon, L. Martin, C.P. Wong, Effect of Ferritic Density and Zinc on Magnetic Properties of Cobalt Ferrite Nanocomposites, in: 11th International Symposium on Advanced Packaging Materials: Processes, Properties and Interface, Atlanta, USA, 2006, pp. 128–131.
[7] R. Lv, F. Kang, J. Gu, X. Gui, J. Wei, K. Wang, D. Wu, Carbon nanotubes filled with ferromagnetic alloy nanowires: Lightweight and wide-band microwave absorber, Appl. Phys. Lett. 93 (2008) 223105.
[8] Y. Yang, M.C. Gupta, K.L. Dudley, Towards cost-efficient EMI shielding materials using carbon nanostructure-based nanocomposites, Nanotechnology 18 (2007) 345701–345704.
[9] Z.H. Hua, R.S. Chen, C.L. Li, S.G. Yang, M. Lu, B.X. Gu, Y.W. Du, $CoFe_2O_4$ nanowire arrays prepared by template-electrodeposition method and further oxidization, J. Alloys Compd. 427 (2007) 199–203.
[10] N. Keller, C. Pham-Huu, C. Estournès, J.-M. Grenèche, G. Ehret, M.J. Ledoux, Carbon nanotubes as a template for mild synthesis of magnetic $CoFe_2O_4$ nanowires, Carbon 42 (2004) 1395–1399.
[11] Z. Wang, X. Liu, M. Lv, P. Chai, Y. Liu, X. Zhou, J. Meng, Preparation of One-Dimensional $CoFe_2O_4$ Nanostructures and Their Magnetic Properties, J. Phys. Chem. C 112 (2008) 15171–15175.
[12] M. Sangmanee, S. Maensiri, Nanostructures and magnetic properties of cobalt ferrite (CoFe2O4) fabricated by electrospinning, Appl. Phys. A 97 (2009) 167–177.
[13] E. Santala, M. Kemell, M. Leskelä, M. Ritala, The preparation of reusable magnetic and photocatalytic composite nanofibers by electrospinning and atomic layer deposition, Nanotechnology 20 (2009) 035602 (5pp).
[14] W.E. Teo, S. Ramakrishna, A review on electrospinning design and nanofibre assemblies, Nanotechnology 17 (2006) R89–R106.
[15] X.-L. Xie, Y.-W. Mai, X.-P. Zhou, Dispersion and alignment of carbon nanotubes in polymer matrix: A review, Mat. Sci. Eng. R 49 (2005) 89–112.
[16] S. Mazinani, A. Ajji, C. Dubois, Morphology, structure and properties of conductive PS/CNT nanocomposite electrospun mat, Polymer 50 (2009) 3329–3342.
[17] K.K.H. Wong, M.Z. -Allmang, J.L. Hutter, S. Hrapovic, J.H.T. Luong, W. Wan, The effect of carbon nanotube aspect ratio and loading on the elastic modulus of electrospun poly(vinyl alcohol)-carbon nanotube hybrid fibers, Carbon 47 (2009) 2571–2578.
[18] A. Yang, X. Tao, R. Wang, S. Lee, C. Surya, Room temperature gas sensing properties of SnO2/multiwall-carbon-nanotube composite nanofibers, Appl. Phys. Lett. 91 (2007) 133110.
[19] S. Aryal, C.K. Kim, K.W. Kim, M.S. Khil, H.Y. Kim, Multi-walled carbon nanotubes/TiO_2 composite nanofiber by electrospinning, Mat. Science and Eng. C 28 (2008) 75–79.
[20] P. Lu, Q. Huang, D. Jiang, B. Ding, Y.-L. Hsieh, I.A. Ovid'ko, A. Mukherjee, Highly Dispersive Carbon Nanotube/Alumina Composites and their Electrospun Nanofibers, J. Am. Ceram. Soc 92 (2009) 2583–2589.
[21] B.D. Cullity, S.R. Stock, Elements of X-ray Diffraction, third ed., Printice-Hall, Englewood Cliffs, 2001.
[22] S. Ramakrishna, K. Fujihara, W.E. Teo, T.C. Lim, Z. Ma, An Introduction to Electrospinning and Nanofibers, World Scientific, Singapore, 2005.
[23] H. Hou, J.J. Ge, J. Zeng, Q. Li, D.H. Reneker, A. Greiner, S.Z.D. Cheng, Electrospun Polyacrylonitrile Nanofibers Containing a High Concentration of Well-Aligned Multiwall Carbon Nanotubes, Chem. Mater 17 (2005) 967–973.
[24] Z. Zhang, A.J. Rondinone, J.X. Ma, J. Shen, S. Dai, Morphological Template of Aligned Spinel $CoFe_2O_4$ Nanorods, Adv. Mat 17 (2005) 1415–1419.
[25] W. Sigmund, J. Yuh, H. Park, V. Maneeratana, G. Pyrgiotakis, A. Daga, J. Taylor, J.C. Nino, Processing and Structure Relationships in Electrospinning of Ceramic Fiber Systems, J. Am. Ceram. Soc. 89 (2006) 395–407.